Extended Data

Extended data Fig. 1) Detection of intranasally administered hMSCs and hMuse cells in the brain and peripheral blood.

Extended data Fig. 1a.

Three-dimensional light sheet imaging showed that, of 50,000 intranasally administered cells, 62.3±4.5% of mCherry-labeled human MSCs (hMSCs) (n=3) (A) (Supplementary Movie 1) and 69.6±9.1% of mCherry-labeled hMuse cells (n=3) (B) (Supplementary Movie 2) migrated to the olfactory bulb by day 1. By day 7, only 1.2±0.1% of hMSCs remained in the entire brain, including the olfactory bulb (n=3) (C) (Supplementary Movie 3), while 28.9±3.3% of hMuse cells remained widely distributed in the brain, including cortex and hippocampus (n=3) (D) (Supplementary Movie 4). Data were represented as mean ± s.e.m., and were analyzed by two-way ANOVA followed by Sidak's multiple comparisons test.

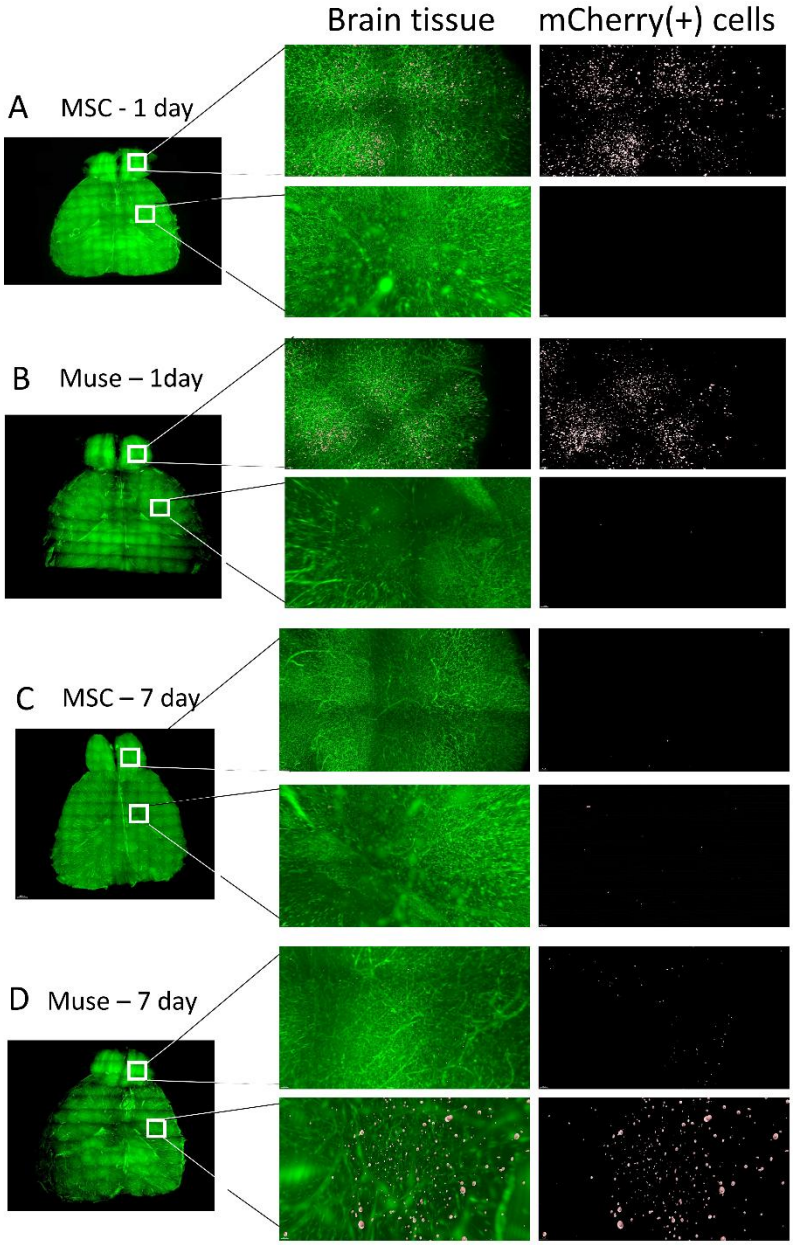

Extended data Fig. 1b.

To investigate whether intranasally administered mCherry(+)-hMSCs and -hMuse cells (both 50.000 cells) exit the brain and leak into systemic circulation after administration, the peripheral blood was subjected to flow cytometric analysis to detect mCherry(+) cells, as reported previously.[1]

1) Representative flow cytometry of mCherry(+)-hMSCs in the peripheral blood, 1, 3, 5 days after nasal administration. Intact animal peripheral blood is the control. mCherry(+)-hMSCs were not detected in the peripheral blood at any time point. n=3 for each time point.

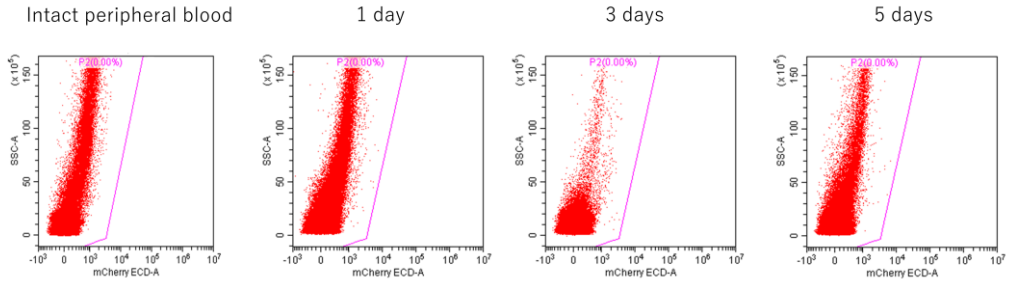

2) Representative flow cytometry of mCherry(+)-hMuse cells in the peripheral blood, 1, 3, 5 days after nasal administration. Intact animal peripheral blood is the control. mCherry(+)-hMuse cells were not detected in the peripheral blood at any time point. n=3 for each time point.

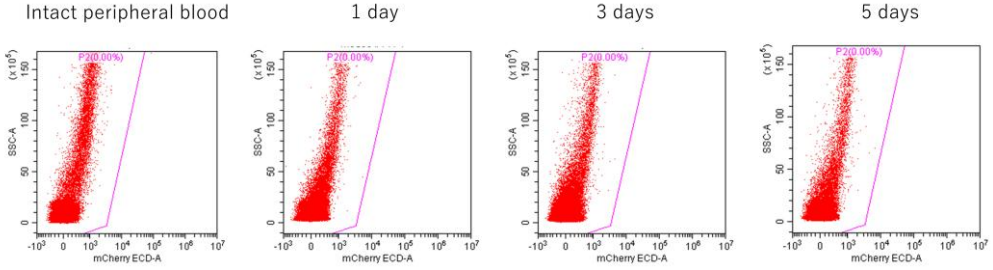

Because Muse cells are home to S1P released from injured tissues,[2] we examined whether intranasally administered Muse cells would exit the brain and enter systemic circulation when administered 1 day after carbon tetrachloride-induced liver damage.[3] Both hMSCs and hMuse cells were examined.

3) Representative flow cytometry of mCherry(+)-hMSCs in the peripheral blood, 1, 3, 5 days after nasal administration. hMSCs were administered 1 day after liver injury. Intact animal peripheral blood is the control. mCherry(+)-hMSCs were not detected in the peripheral blood at any time point. n=3 for each time point.

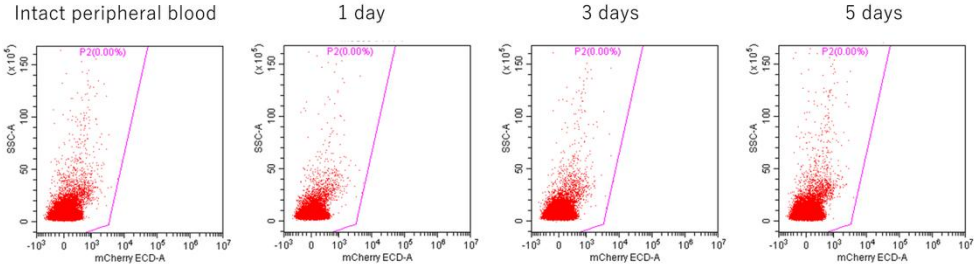

4) Representative flow cytometry of mCherry(+)-hMuse cells in the peripheral blood, 1, 3, 5 days after nasal administration. hMuse cells were administered 1 day after the liver damage. Intact animal peripheral blood is the control. mCherry(+)-hMuse cells were not detected in the peripheral blood at any time point.

n=3 for each time point.

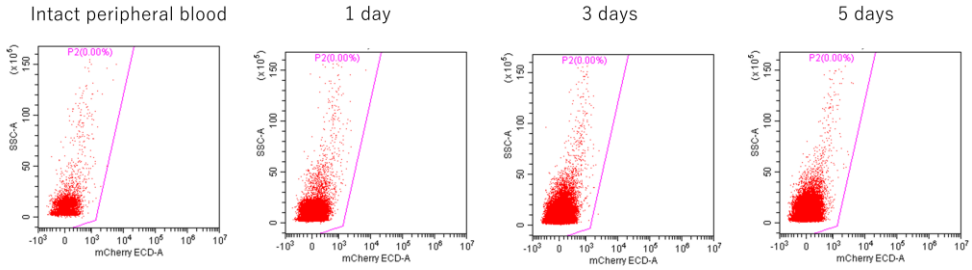

These results suggested that both intranasally administered hMSCs and hMuse cells did not leak from the brain into the systemic circulation, regardless of whether organs other than the brain were acutely injured.

Extended data Fig. 2) Immunohistochemical analysis of the 5xFAD mouse brain after treatment.

Extended data Fig. 2a. Control data for immunohistochemistry.

A negative control for anti-Aβ, -human-mitochondria (h-mitochondria, cytoplasmic), -human-KU80 (h-Ku80, nuclear), -NeuN, -Tuj-1, -neurofilament-M, -APC, -GFAP, and -Iba1 was performed by using the vehicle group sample at 16 weeks. The secondary antibodies used were as follows: Alexa Fluor 488–conjugated donkey anti–mouse IgG (for Aβ), Alexa Fluor 488–conjugated donkey anti–rabbit IgG (for h-mitochondria, h-KU80), Alexa Fluor 594–conjugated donkey anti–mouse IgG (for NeuN, Tuj1, APC, and GFAP), and Alexa Fluor 594–conjugated donkey anti–goat IgG (for Iba1). The specificity of h-mitochondria antibody and neural markers (NeuN and GFAP; both known to react to human and mouse) in mouse brain tissues was confirmed in the previous report using the same antibody.[4] As shown in Fig. 2E, Aβ was detected in the same way as in the original paper on 5xFAD.[5] Negative and positive controls for anti-h-mitochondria and anti-h-Ku80 are shown below. The specific staining pattern of anti-Tuj1, -NeuN, -APC, -GFAP, and -Iba-1, known to react with both human and mouse, was checked in the vehicle group brain (16 weeks), as shown below. Scale bars: 50 μm, n=3 each group.

Negative control, incubated only with secondary antibody, for anti-Aβ, -h-mitochondria, -h-Ku80, -NeuN, -Tuj-1, -APC, -GFAP, and -Iba1 in the vehicle group brain (16 weeks) is shown below. n=3 for each group.

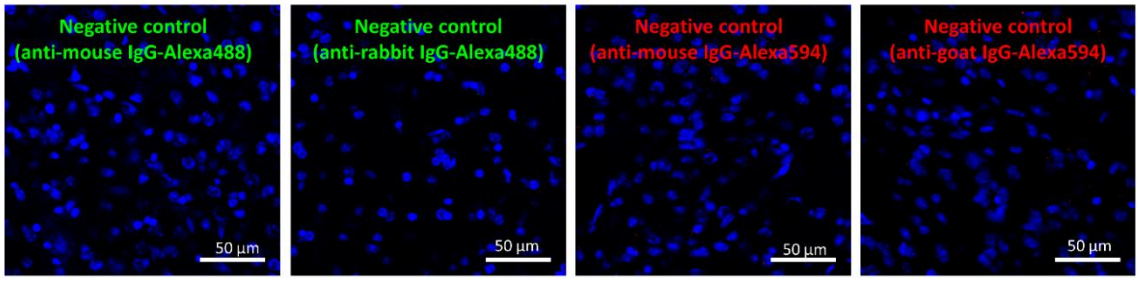

Anti-h-mitochondria and -h-Ku80 were negative in the vehicle group brain (16 weeks). n=3 for each group.

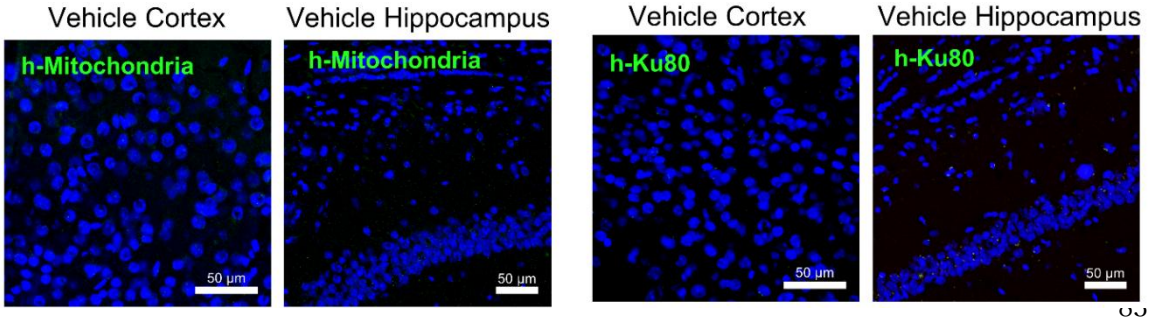

The human umbilical cord tissue confirmed the positivity of h-mitochondria and h-Ku80. Negative control omitted primary antibodies. n=3 for each group.

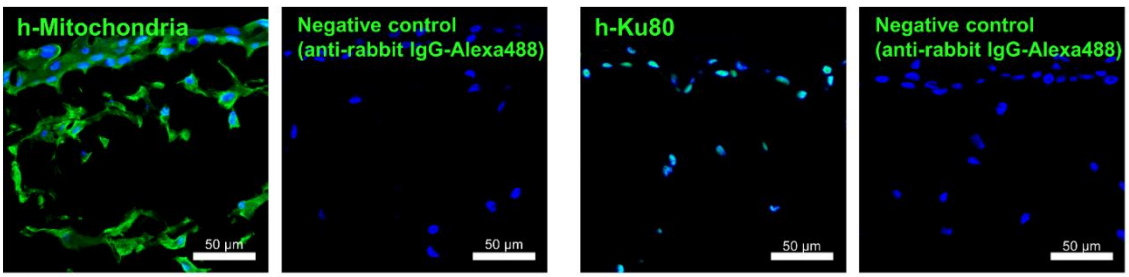

Anti-NeuN, -Tuj1, -APC, -GFAP, and -Iba-1antibodies react to human and mouse. The vehicle group brain (16 weeks) was used to check the staining pattern of those antibodies. n=3 for each group.

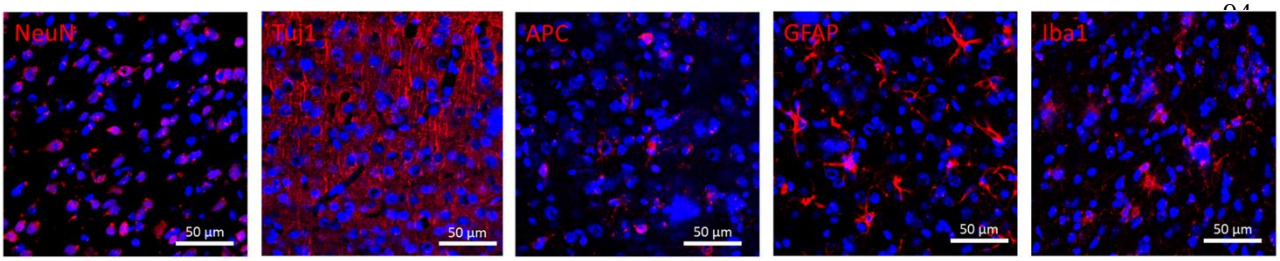

Extended data Fig. 2b. Homing of hMSCs and hMuse cells in the brain (16 weeks).

Estimated engraftment rate of administered h-mitochondria (+) cells in the MSC-Low, MSC-high, Muse-IV, and Muse-IN groups.The number of h-mitochondria (+) cells across the whole area of the coronal sections of the brain from 2 mm anterior to 3 mm posterior to the bregma was counted in a blinded manner, and the mean cell density (number of cells/mm^2) was calculated using ImageJ. Then, the estimated engraftment rate of the administered cells in the whole brain was calculated based on h-mitochondria(+) cell counts as previously described (Supplementary Method 1).[2] Bars were expressed as the mean ± standard deviation (SD). One-way analysis of variance (ANOVA) followed by Tukey-Kramer honestly significant difference (HSD) test was used. n=3 for each group. ***: p<0.001.

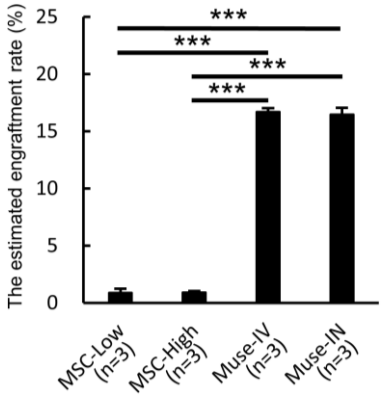

Extended data Fig. 2c. hMuse cell homing to the cortex and hippocampus (16 weeks).

Number of h-mitochondria (+) cells/mm^2 in the cortex and hippocampus of the Muse-IV and Muse-IN groups. For each sample, images of randomly selected 20 areas (250 × 250 μm each) were taken from the cortex and hippocampus of both hemispheres and were analyzed in a blinded manner. Bars were expressed as the mean ± SD. An unpaired Student's t-test was used. n=3 for each group. *: p<0.05, **: p<0.01.

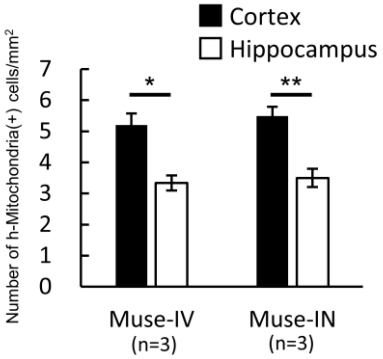

Extended data Fig. 3) Validation of human-specific *Alu* sequence by droplet digital polymerase

To establish a highly sensitive and quantification method for detecting human cells in mouse brain tissue, the sensitivity of a human-specific *Alu* ddPCR assay was done.

(A) One-dimensional amplitude dot plots for human *Alu* droplets. Plots are shown for serial dilutions of human genomic DNA (gDNA) (100 pg, 10 pg, 1 pg, and 0.1 pg) spiked into mouse gDNA (10 ng) to simulate the experimental sample environment, as well as a no template control (NTC) containing nuclease-free water. The fluorescence threshold for positive droplets was manually set at 7,000 relative fluorescence units across all samples to ensure consistent quantification. n=3 for each group.

(B) Standard curve generated from the ddPCR data. The curve was constructed by subtracting the mean *Alu* copy number of the mouse-only gDNA samples from each dilution point. The total number of human *Alu* copies per 20 µL reaction is plotted against the input amount of human gDNA (pg). The regression line (y = 201.1x -24.9) demonstrates high linearity with a coefficient of determination (R^2) of 0.999. Data were expressed as the mean ± SD. n=3 for each group. Linear regression analysis was performed based on the least squares method.

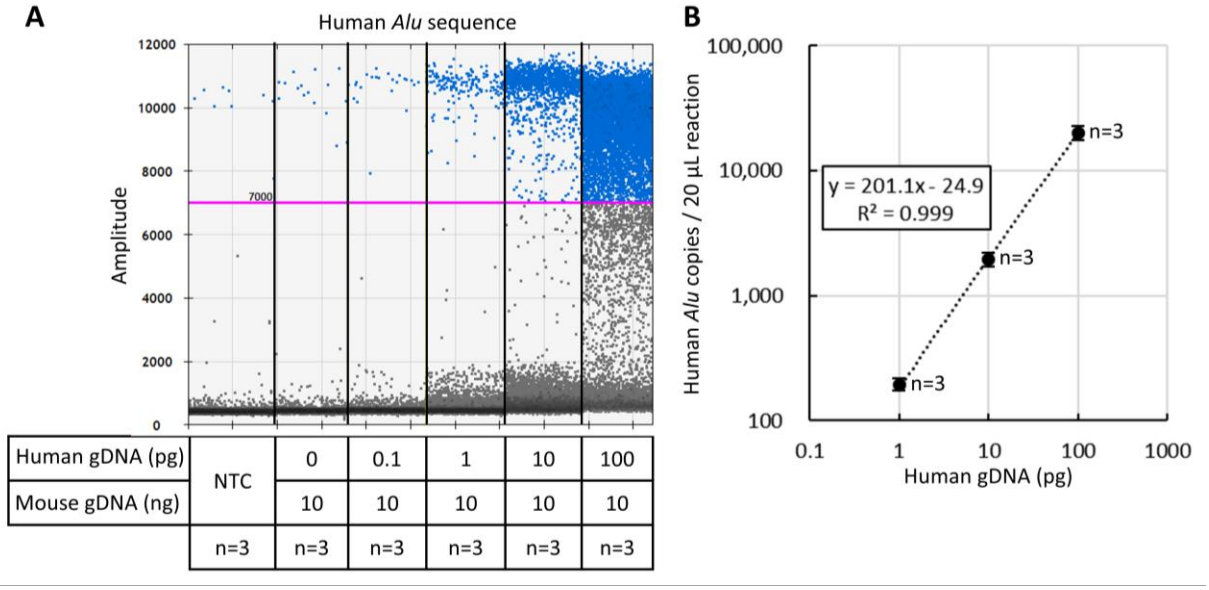

Human gDNA (pg)	NTC	0	0.1	1	10	100
Mouse gDNA (ng)		10	10	10	10	10
	n=3	n=3	n=3	n=3	n=3	n=3

Extended data Fig. 4) The effect of Aβ and p-Tau on hMuse cells.

Extended data Fig. 4a) Exposure to Aβ.

Since the 5xFAD mouse is an amyloid-β (Aβ) pathology model characterized by both intraneuronal and extracellular Aβ aggregations,[5] the effect of Aβ on hMSCs, naïve hMuse cells (n-Muse), and neuronal differentiated hMuse cells (Neuro-Muse) was examined. Neuro-Muse cells were induced through phagocytosis-dependent differentiation, as described previously (see Method).[6] In brief, mouse neuronal cells were collected from a primary culture of neonatal (P1) C57BL/6 brain, treated with 100 μM antimycin A for 1 day to induce apoptosis, collected apoptotic fragments, labelled with PKH 26, and were supplied to n-Muse cells to induce phagocytosis-dependent neuronal differentiation.[6] As reported, hMuse cells were shown to phagocytose PKH26 Red-labeled apoptotic neural fragments at 24 hrs.[6] Engulfed PKH26 (+) fragments merged with LAMP-1, lysosomal marker, in hMuse cell cytoplasm, suggesting phagocytosis. The specificity of LAMP-1 has been confirmed previously.[6]

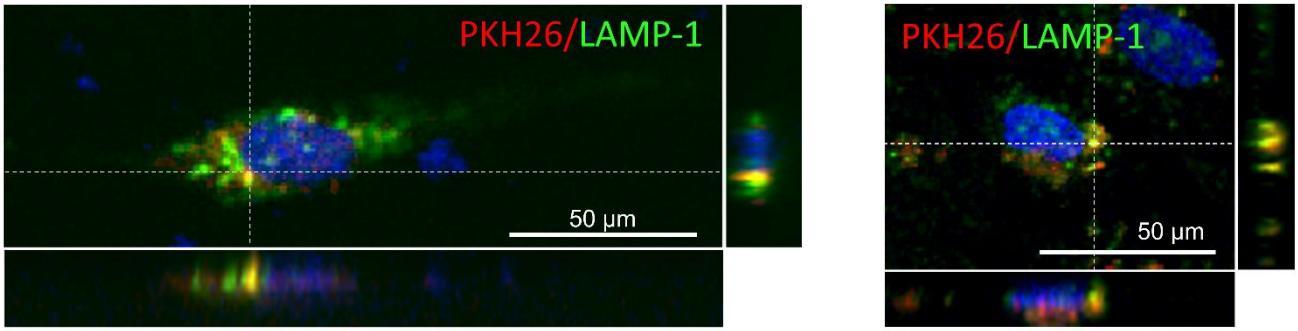

Neuro-Muse expressed neurofilament-M at 21 days, as shown below, similar to the previous report.[6] The specificity of neurofilament-M has been confirmed previously.[6] hMSCs, n-Muse, and Neuro-Muse (at 21 days of induction) were cultured with or without 1 μM Aβ in Neurobasal medium plus B27 supplement for 5 days, and were subjected to TUNEL-staining. The positive control for TUNEL was done by treating hMSCs with DNase, and the negative control without TdT. PC12 cells were used as a positive control for Aβ-induced cell death.[7]

Small number of TUNEL(+) were detected among MSCs, n-Muse, and Neuro-Muse, regardless of whether Aβ was present or absent, and there was no statistical significance among the three (n=3 each group). In PC12, TUNEL-positive cells were substantially increased by Aβ exposure (n=3). PC12 was used only to verify Aβ is active to induce neuronal cell death and was not used as a comparative reference; accordingly, no statistical analysis was performed. One-way ANOVA followed by Tukey-Kramer HSD test was used for statistical analysis. Data represent the mean ± SD.

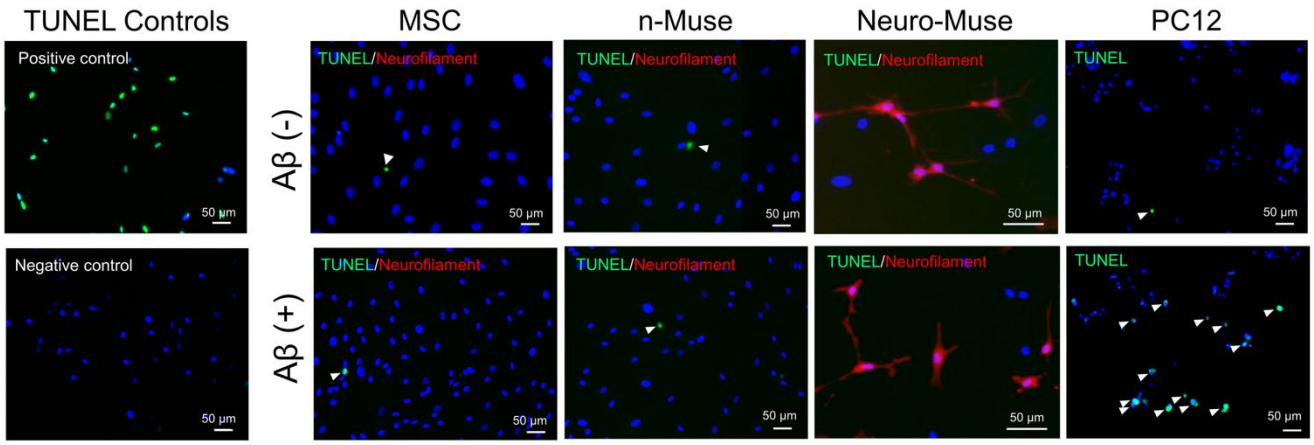

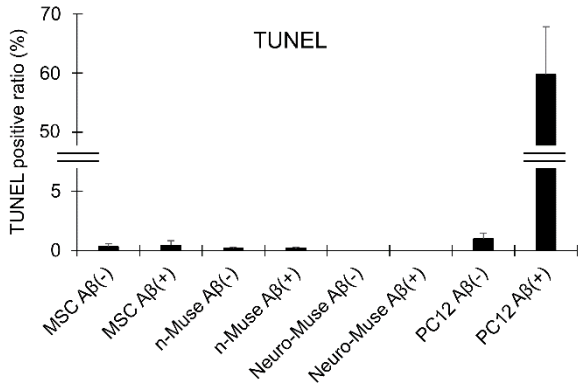

Extended data Fig. 4b) Effect of p-Tau on neuronal differentiation.

In AD, including the 5xFAD model, phosphorylated tau (p-tau), which leads to cell death, accumulates in neurons in the presence of neurotoxic Aβ aggregates.[5] On the other hand, P-tau can be dephosphorylated by the protein phosphatase 1/2 catalytic subunit alpha (PPP1CA, PPP2CA).[8]

(1) hMuse cells were suggested to express higher gene levels of PPP1CA and PPP2CA than normal human cortical and hippocampal neurons. Bulk RNA sequence data of PPP1CA and PPP2CA expressions in normal human adult brain cortex (n=270),[9] hippocampus (n=255),[9] and in hMuse cells (n=3) are shown below. A one-way ANOVA followed by Tukey-Kramer HSD test was used. Data represent the mean ± SD. ***: p<0.001.

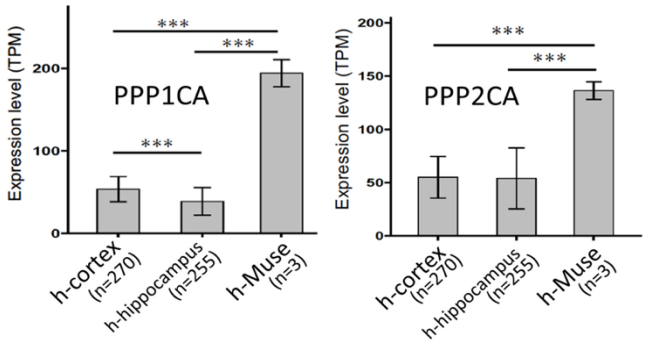

(2) Muse cells utilize factors (e.g., transcription factors) after phagocytosing dead cell fragments and differentiate into the same cell types.[6] However, in AD, apoptotic neuronal cell fragments contain

neurotoxic p-tau.[10] To examine whether Muse cells retain neuronal differentiation after phagocytosing p-tau containing neuronal fragments, we examined as follows: mouse neuronal cells were collected from a primary culture of neonatal (P1) C57BL/6 brain (panel ①), treated with 1 μM Aβ for 5 days to induce apoptosis (panel ②), additionally treated with 100 μM antimycin A for 1 day to accelerate apoptosis, and apoptotic fragments were collected. These fragments were supplied to naïve hMuse cells to induce phagocytosis-dependent neuronal differentiation, as described previously.[6] h-Muse cells at day 7 (panel ③) and day 21 (panel ④) incubation showed similar results to a previous report.[6] On day 21, samples were collected as Neuro-Muse cells, and were analyzed.

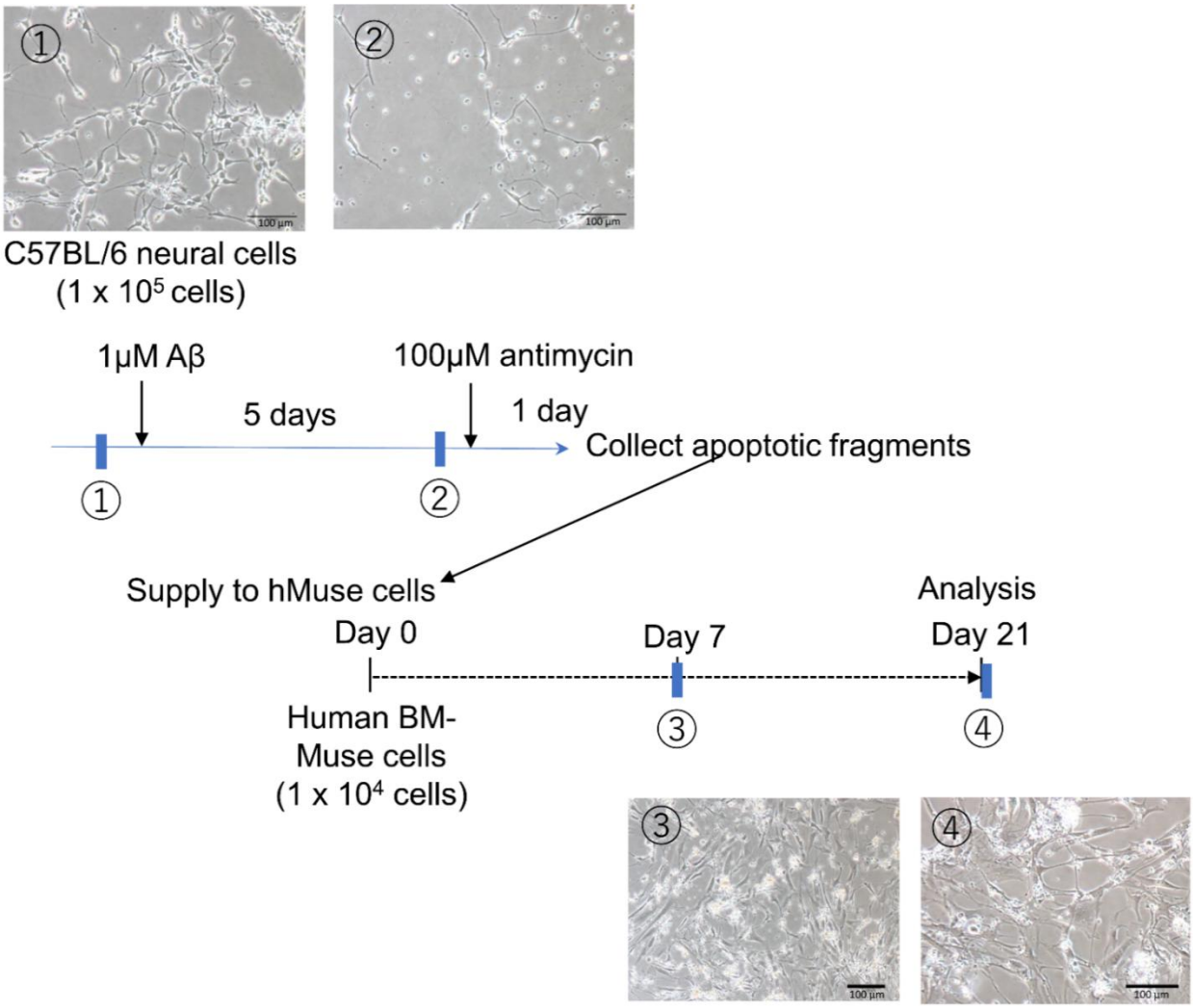

(3) The figure below shows a Western blotting for total-Tau (t-Tau) and p-Tau in C57BL/6 neonate brain (P1)-derived neural cells cultured without [Aβ (-)] and with [Aβ (+)] (5 days), naïve human Muse cells (n-Muse), and Neuro-Muse cells (Neuro-Muse). Beta-actin (ACTB) is used as an internal control. Following exposure to Aβ for 5 days in vitro, the expression level of t-Tau did not differ between Aβ (-) and Aβ (+) neonatal mouse brain-derived neural cells, but p-Tau increased only in Aβ (+) neonatal neural cells ($p<0.05$). In hMuse cells, t-Tau was elevated in Neuro-Muse cells rather than in n-Muse cells ($p<0.05$). However, p-Tau did not elevate in Neuro-Muse cells compared to n-Muse cells. The experiment was repeated three times. Data were analyzed using one-way ANOVA followed by the Tukey–Kramer HSD test for comparisons among the four groups. Data represent the mean ± SD. n=3 for each group. *: $p<0.05$, ***: $p<0.001$.

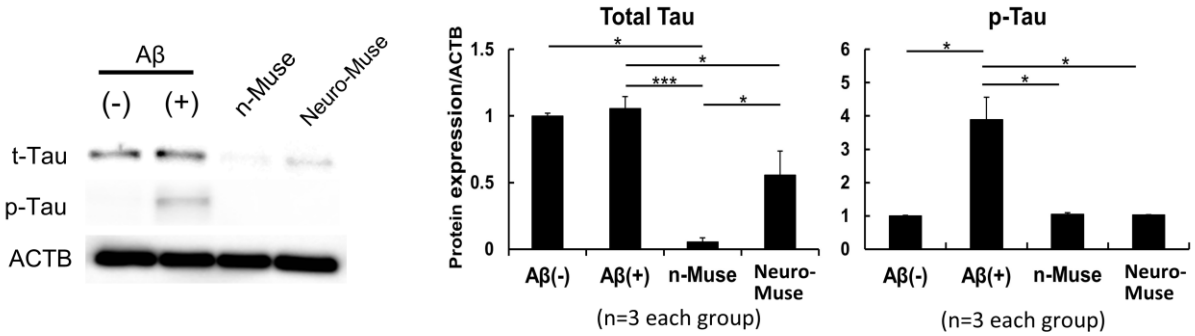

Original gel images.

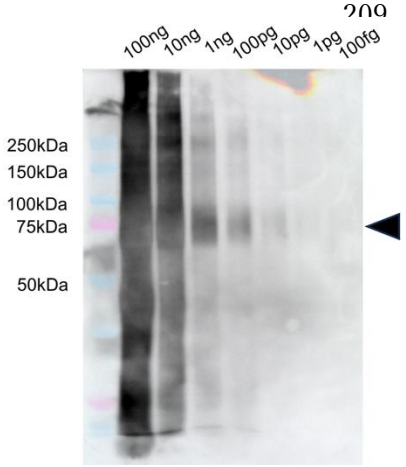

Positive control for anti-p-Tau in Western blotting.

A quality check of the anti-p-Tau (phosphorylated T231) positive control using recombinant human p-Tau (Thr 231) protein (Biorbyt, #orb1974299) showed a positive band at 70~75 kDa, with intensity increasing across the concentration gradient.

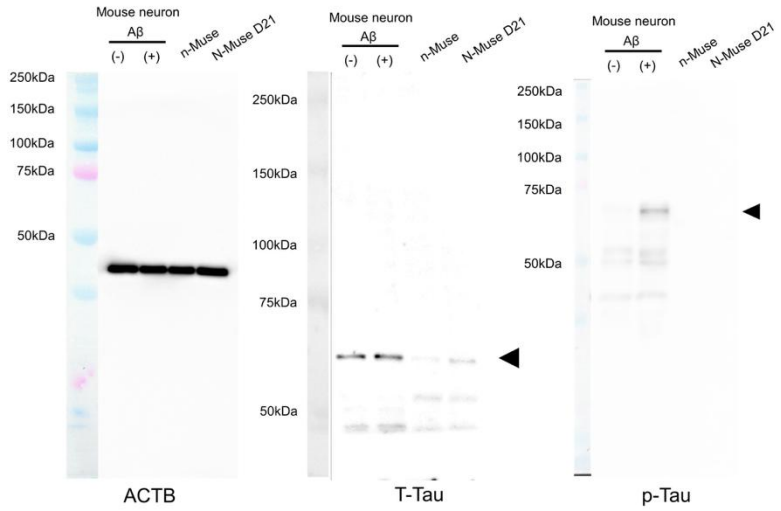

Whole gel images of beta-actin (ACTB), t-Tau, and p-Tau.

(4) Quantitative polymerase chain reaction (q-PCR) for human-specific MAP2, NeuN, PPP1CA, and PPP2CA in naïve-human Muse cells (n-Muse), Neuro-Muse cells (Neuro-Muse), positive control (human fetus whole total RNA), and negative control (apoptotic mouse neural cell fragments). The positive control was used only to verify that the target could be detected by the assay and was not used as a comparative reference; accordingly, no statistical analysis was performed. N-Muse cells, negative for human-MAP2 and -NeuN, expressed these markers as differentiated into Neuro-Muse (both; $p<0.001$). On the other hand, human-PPP1CA and -PPP2CA expression levels did not show significant difference between n-Muse and Neuro-Muse. The experiment was repeated three times. An

unpaired Student's t-test was used to assess the significance between the n-Muse and Neuro-Muse groups. Data represent the mean ± SD. n=3 for each group. ***: p<0.001.

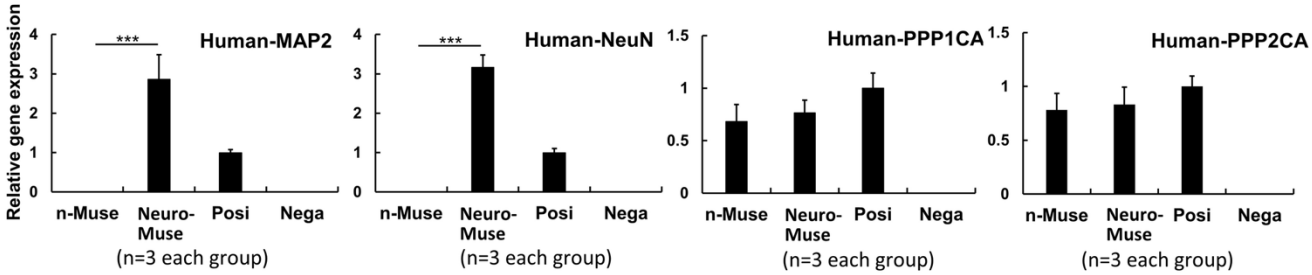

(5) Western blotting confirmed that PPP1CA and PPP2CA expression levels did not show statistical significance among human-MSCs (h-MSC), -naïve Muse cells (n-Muse), and -neuro-Muse cells (Neuro-Muse). HeLa cells were used as a positive control (Posi).[11] The positive control was used only to verify that the target could be detected by the assay and was not used as a comparative reference; accordingly, no statistical analysis was performed. The experiment was repeated three times. One-way ANOVA followed by Tukey-Kramer HSD test was used for statistical analysis. Data represent the mean ± SD. n=3 for each group.

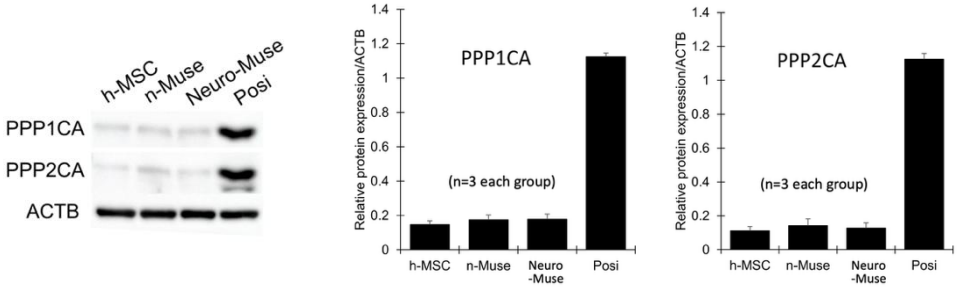

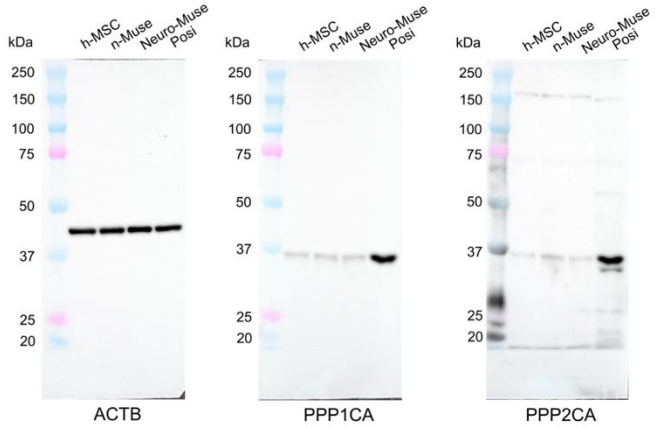

Original gel images

Overall, these data suggested that survival and neuronal differentiation of Muse cells were not significantly impaired despite the presence of Aβ and p-Tau in vitro.

Extended data Fig. 5) Neural and microglial marker expression in hMuse cells (16 weeks).

In the Muse-IV cortex (both hemispheres), 44.8 ± 8.2 % (the mean ± SD) of h-mitochondria (+) cells were NeuN (+), 14.8 ± 2.0 % were APC (+), 6.8 ±1.9 % were Iba-1 (+), while few cells were positive for GFAP. Similarly, the Muse-IN cortex (both hemispheres) showed that 51.1 ± 5.3 % of h-mitochondria (+) cells were NeuN (+), 13.0 ± 0.4 % were APC (+), 6.5 ± 3.3 % were Iba1 (+), while few cells were positive for GFAP. There was no statistical difference between the two groups in the percentage of markers positive (Fig. 2A), as analyzed by an unpaired Student's t-test. n=3 for each group.

Extended data Fig. 5a) GFAP expression in the Muse-IN brain.

Few h-mitochondria (+) Muse cells expressed GFAP. White arrowhead shows h-mitochondria(+) cells (green) negative for GFAP (red).

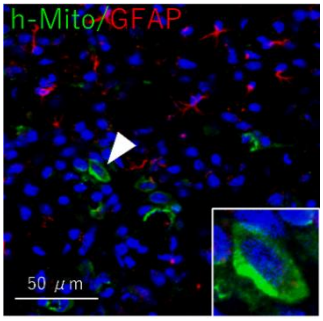

Extended data Fig. 5b) Marker expression in the Muse-IV brain.

NeuN, APC, and Iba1 were expressed in h-mitochondria (+) Muse cells, while a few cells expressed GFAP.

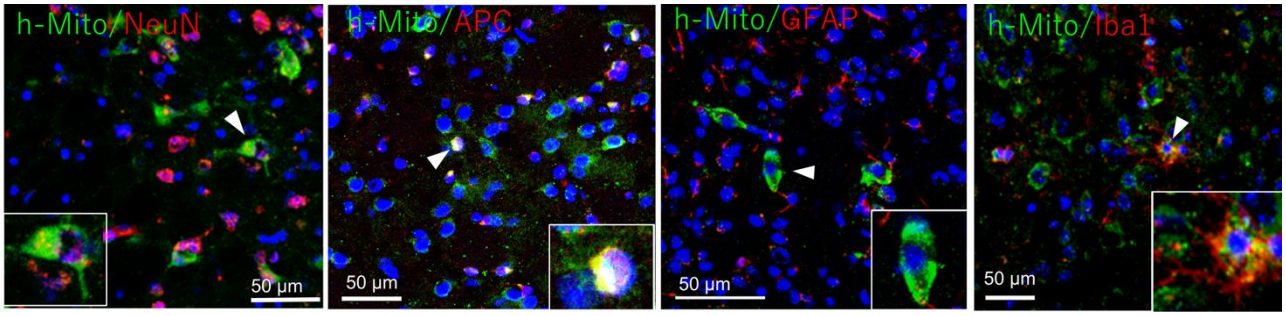

Extended data Fig. 5c) Marker expression in h-Ku80 (+) cells in the Muse-IN and Muse-IV brains.

h-Ku80/Tuj1 and h-Ku80/GFAP are from the Muse IN group, and h-Ku80/APC and h-Ku80/Iba1 are from the Muse IV group.

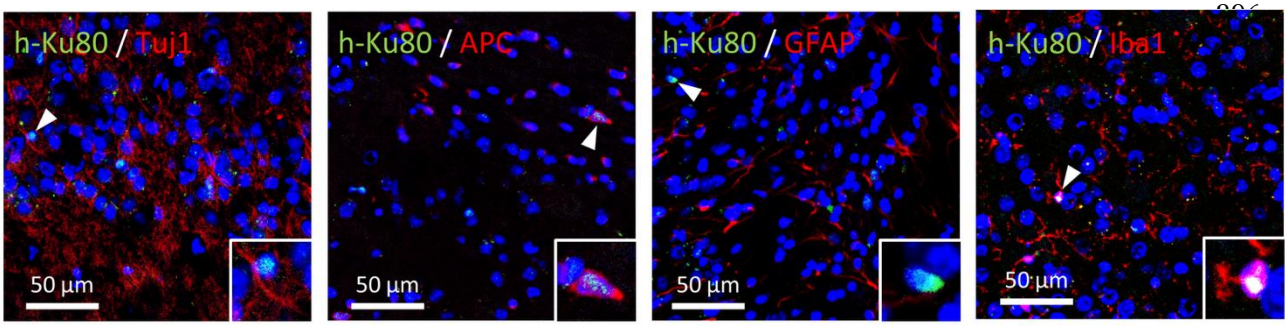

Extended data Fig. 6) Histological analysis of organs at 16 weeks.

Tumor formation was not observed in the brain (Fig. 1C-1E, 2B-2E), lungs, liver, kidneys, testes, pancreas, and small and large intestines in all five groups in hematoxylin-eosin staining. n=10 for each group. Representative images of each organ were shown.

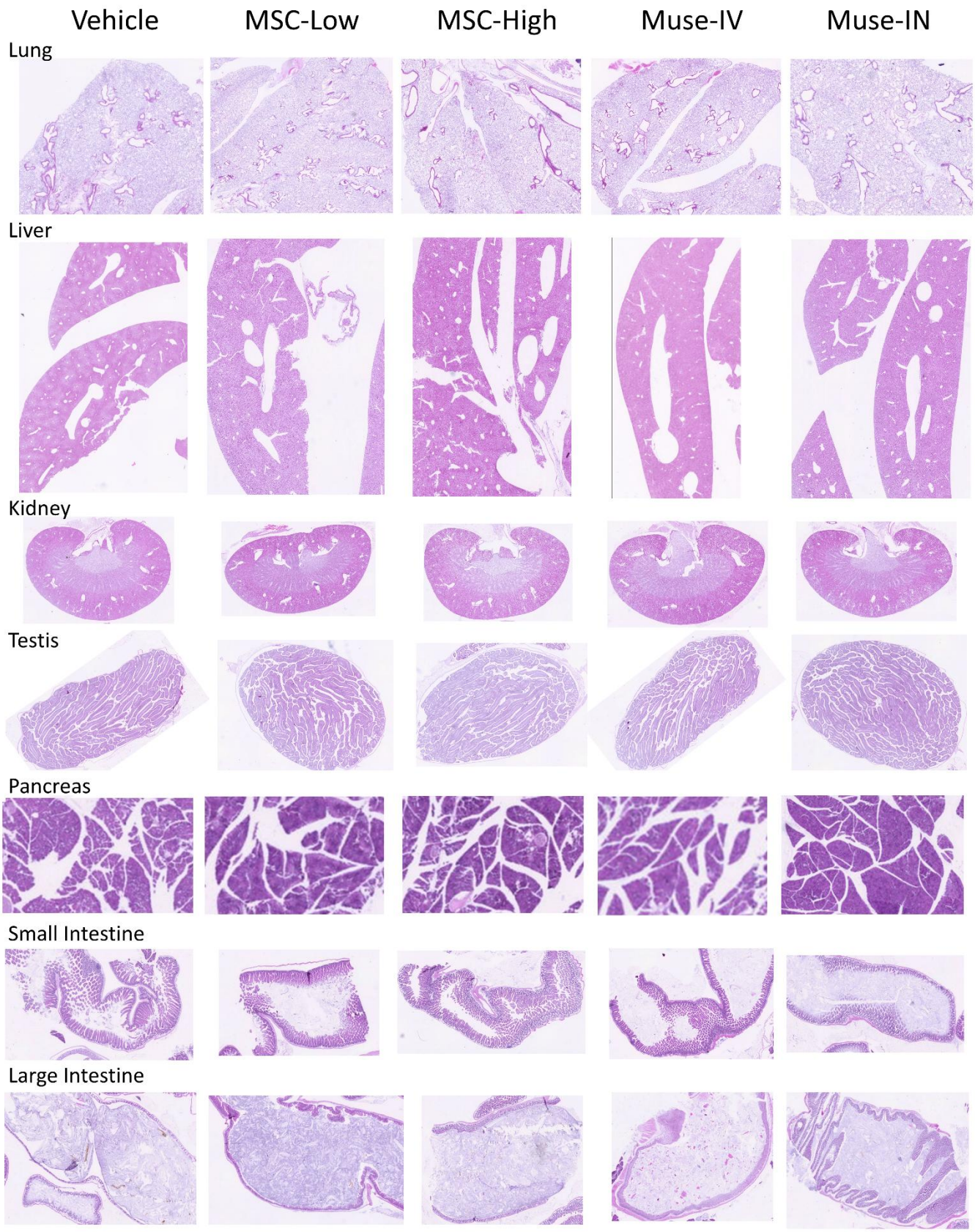

Extended data Fig. 7) Analysis of Aβ in the brain at 16 weeks.

(A) The percent area occupied by Aβ plaques, measured by ImageJ, was largest in the vehicle group, intermediate in the MSC-Low and MSC-High groups, and significantly smaller in the Muse-IV and Muse-IN groups, with no significant difference between the Muse-IV and Muse-IN groups (see Fig. 2E). In each sample, randomly selected 20 areas (250 × 250 μm each) were taken from the cortex and hippocampus of both hemispheres, and were analyzed in a blinded manner with ImageJ. The values (mean ± SD) were expressed as Aβ (% area). One-way ANOVA followed by Tukey-Kramer HSD test was used. n=3 for each group. *; p<0.05, **; p<0.01, ***; p<0.001.

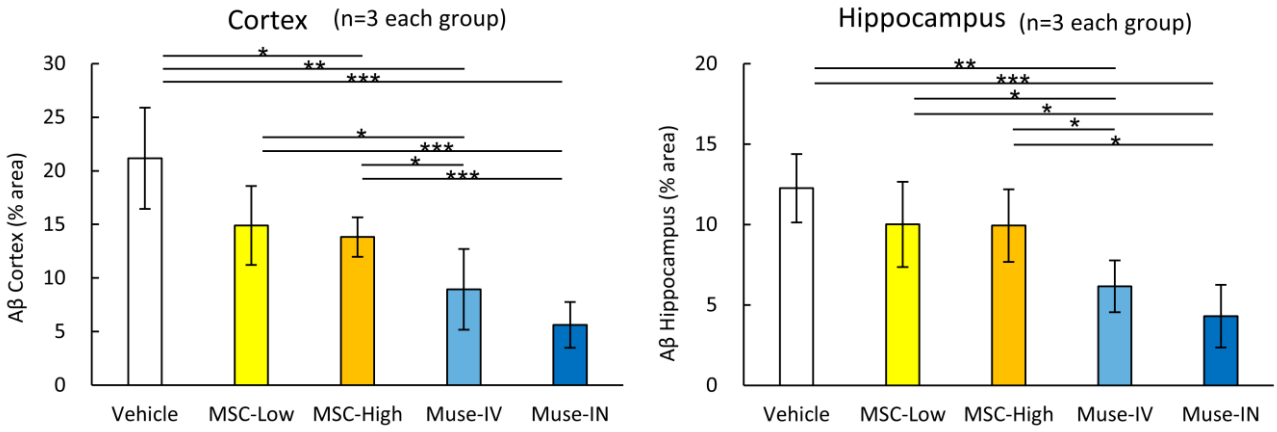

(B) The size of each Aβ aggregate, measured by ImageJ, in the cortex and hippocampus showed no significant differences among the five groups (see Fig. 2E). In each sample, randomly selected 20 areas (250 × 250 μm each) were taken from the cortex and hippocampus of the both hemispheres, and were analyzed in a blinded manner with ImageJ. The values (mean ± SD) were expressed as the size of the Aβ plaque (μm). One-way ANOVA followed by Tukey-Kramer HSD test was used. n=3 for each group.

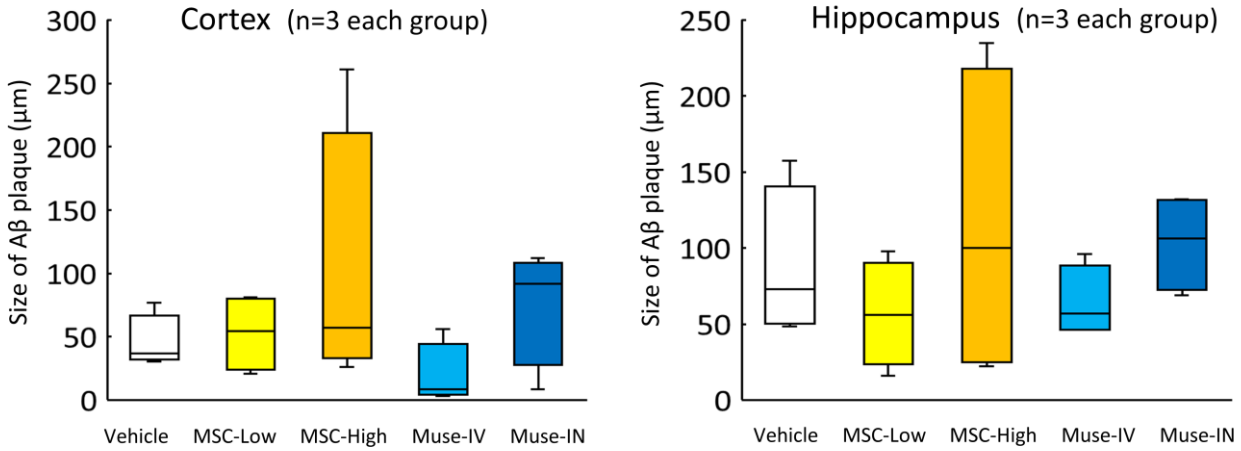

Extended data Fig. 8) Correlation between Aβ plaques and microglia (16 weeks).

To evaluate a potential clearance mechanism, the correlation between Aβ plaque % area and the total number of microglial marker Iba1(+) cells per area was examined in the five groups, because microglial cells clear Aβ plaques[12] and Muse cells differentiated into Iba1(+) cells as shown in Fig. 2A and 2D. In the 5xFAD mouse model, a strong correlation between Aβ plaques and microglial cells was observed in the cortex, where neuronal loss is greater than in the hippocampus.[5]

For both Iba1(+) cells/mm^2 and Aβ plaque (% area) counting, 20 randomly selected areas (250 × 250 μm each) were taken from the cortex and hippocampus of both hemispheres and analyzed in a blinded manner with ImageJ. Correlations were assessed using the Pearson correlation coefficient, which indicated a strong correlation between Aβ plaque and Iba1 (+) cell density in the cortex. n=3 for each group.

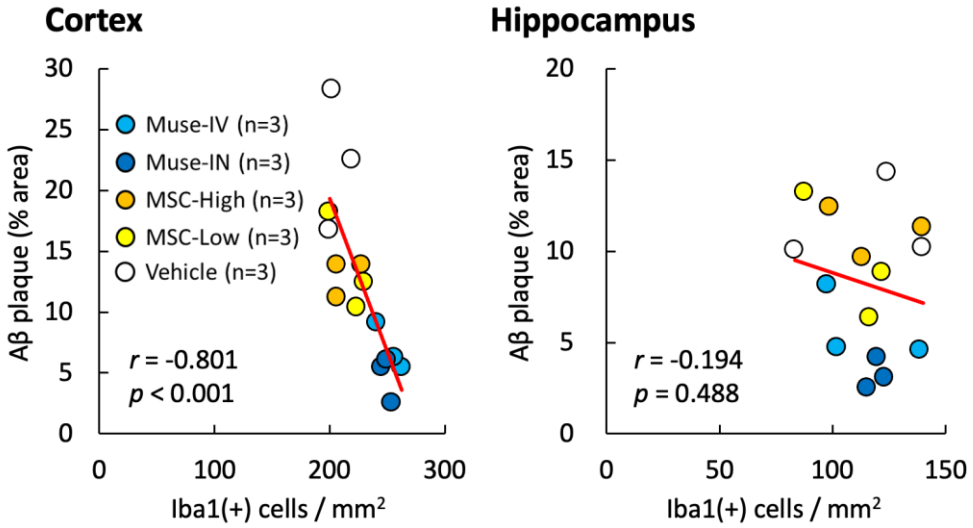

Extended data Fig. 9) Scanning X-ray fluorescence microscopic analysis (16 weeks).

Aβ aggregation is known to disrupt metal homeostasis in the brain, as indicated by the association of metal-rich aggregates with amyloid plaques.[13] The distribution of Fe and Cu in the piriform cortex, where Aβ plaques were abundantly observed in the vehicle group (A), was analyzed. Scanning X-ray fluorescence microscopy showed reduced Fe and Cu levels in Muse-IN brains (B). The percent of fluorescence intensity of the Fe (C) and Cu (D) was significantly lower in the piriform cortex of the Muse-IN group than in the vehicle group. Randomly selected five regions (each 5×5 μm) in the cortex were analysed in a blind manner. Data represent the mean ± SD. An unpaired Student's t-test was used. n=3 for each group. ***; p<0.001.

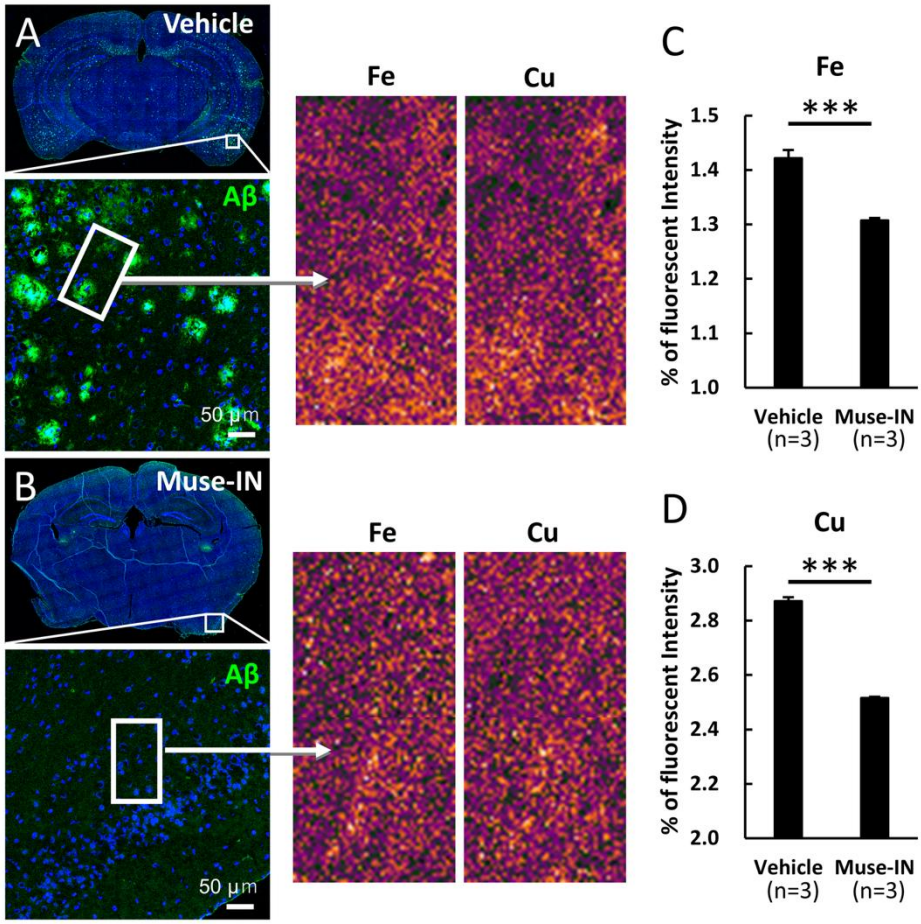

Extended data Fig. 10) Analysis of gliosis (16 weeks).

Gliosis begins at ~2 months after birth in the 5xFAD mouse.[5] The extent of gliosis in the five groups was examined by GFAP staining at 16 weeks. For each sample, images of randomly selected 20 areas (250 × 250 μm each) were obtained from the cortex and hippocampus of both hemispheres and analyzed in a blinded manner with ImageJ. The mean values (mean ± SD) were calculated and expressed as GFAP (+) cells/mm^2. One-way ANOVA followed by Tukey's HSD test. n=3 for each group. *; p<0.05, **; p<0.01, ***; p<0.001.

GFAP staining (red signal)

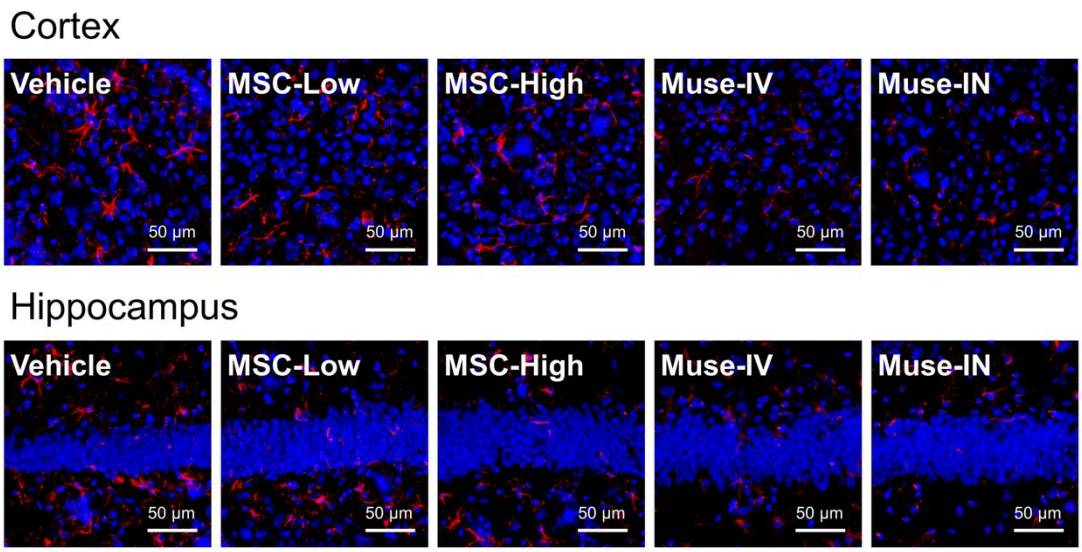

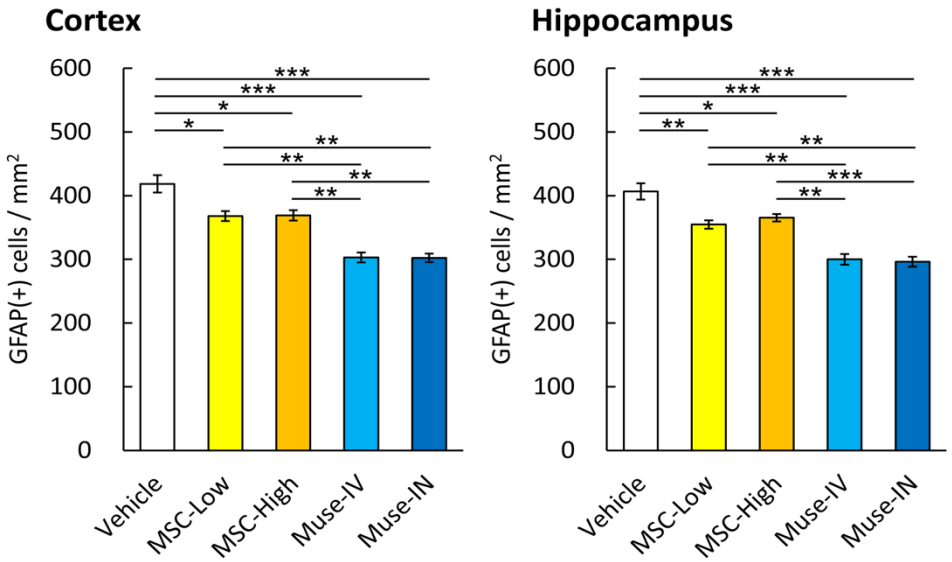

Supplementary Methods

Supplementary Method 1.

Calculating the estimated ratio of h-MSCs and h-Muse cells integrated into the brain.

The engraftment rate of the administered cells in the whole brain was estimated as follows, as described previously[2]: the brain was sectioned into six coronal slices based on their distance from the bregma. Slices at +2 mm and 0 mm from the bregma were 2 mm thick, while the remaining slices were 1 mm thick. All six slices were embedded in OCT compound, and the tissue blocks were sectioned at 10 μm. H-mitochondria(+) cells were detected by immunofluorescence staining, and their numbers were counted across the entire tissue section area. While the diameters of the h-mitochondria(+) cells ranged from 10 to 20 μm, we assumed a diameter of 20 μm for h-mitochondria(+) cells to prevent overestimation. As illustrated below, a 20-μm-thick section may contain h-mitochondria(+) cells at various depths. Therefore, the number of cells counted in a single section may reflect the number of h-mitochondria(+) cells within a 60-μm depth in each section (thickness of the section and 20 μm above and below that section; refer to the figure below). Consequently, 1-mm thick slices were calculated to contain 16.7 times the number of cells counted in a single cryosection, while 2-mm thick slices were considered to contain 33.3 times that number. The estimated total number of engrafted cells was then determined by summing the counts from six slices. Finally, the engraftment rate of the administered cells in the whole brain was estimated based on this total.

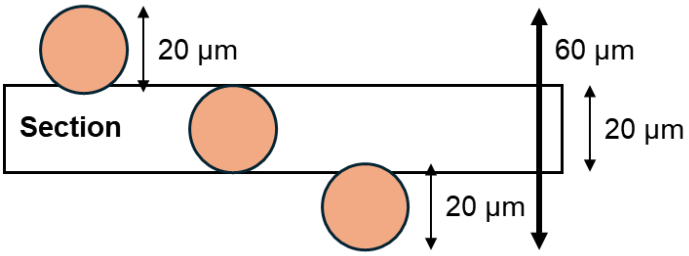

Supplementary Method 2.

Human-specific primers for qPCR.

human NEUN-F	TACGCAGCCTACAGATACGCTC
human NEUN-R	TGGTTCCAATGCTGTAGGTCGC
human PPP1A-F	GGCGTCTCTTTTACCTTTGGAGC
human PPP1A-R	GGAGCTGAGAAAAGTGTCACCAG
human PPP2CA-F	GGTGGTCTCTCGCCATCTATAG
human PPP2CA-R	CTGGATCTGACCACAGCAAGTC
human MAP2-F	AGGCTGTAGCAGTCCTGAAAGG
human MAP2-R	CTTCCTCCACTGTGACAGTCTG
human ACTB-F	CACCATTGGCAATGAGCGGTTC
human ACTB-R	AGGTCTTTGCGGATGTCCACGT

References

1. Sato, T.*, et al. Cell Transplant* **29**, 963689720923574 (2020).
2. Yamada, Y.*, et al. Circ Res* **122**, 1069-1083 (2018).
3. Iseki, M.*, et al. Cell Transplant* **26**, 821-840 (2017).
4. Yamamoto, S.*, et al. Sci Rep* **15**, 16243 (2025).
5. Oakley, H.*, et al. J Neurosci* **26**, 10129-10140 (2006).
6. Wakao, S.*, et al. Cell Mol Life Sci* **79**, 542 (2022).
7. Tong, Y.*, et al. Sci Rep* **8**, 26 (2018).
8. Liu, F., *et al. Eur J Neurosci* **22**, 1942-1950 (2005).
9. Consortium, G.T. *Science* **369**, 1318-1330 (2020).
10. Choi, H.J.*, et al. Mol Brain* **15**, 63 (2022).
11. Torres, J.Z., *et al. Mol Biol Cell* **21**, 897-904 (2010).
12. Brown, M.R.,*et al*. *Front Mol Neurosci* **13**, 609073 (2020).
13. Everett, J.*, et al. Nanoscale* **10**, 11782-11796 (2018).